

General Probabilistic Bounds for Trajectories using only Mean and Variance

Cheng Fang¹ and Brian C. Williams¹

Abstract—Two ideas have gained traction in research in the robotics planning community. Activity planning has become popular where a library of predefined manipulation of the vehicle state is accessible, and is commonly used for missions with complex goal specifications. Another focus has been chance-constrained programming as a method of providing robust motion planning, in which the probability of failure is bounded. A combination of the two would allow for robust satisfaction of complex directives.

However, to perform chance-constrained activity planning, we must be able to provide probabilistic bounds on the trajectory of the vehicle. While this may be done through propagation of statistics, we would require information about the actuation noise for the vehicle dynamics. In addition to such parameters as mean and variance, we also need to know the appropriate function for the noise.

In many cases, the exact distribution of the actuation noise may not be known, although researchers can easily approximate the first two moments through calibrations. In this work we look at statistics propagation when only the first two moments of the actuation uncertainty is known, assuming white noise. We show that for linear systems, propagation is exact. Further, by looking at the expected error squared as a stochastic process, we can show that it is a submartingale under certain assumptions, and thus derive error bounds for deviation from mean over the duration of the entire path. We empirically show that, for nonlinear dynamics, we may approximate the propagation with the unscented transform, and obtain the corresponding bounds.

I. INTRODUCTION

The vision for robotics planning is a suite of intelligent algorithms which would be able to robustly achieve complex human specified goals. This is motivated by such diverse scenarios as autonomous manufacturing with robotic arms [1] and the use of robotic vehicles in oceanography [2] (Figure 1). There thus exists two subproblems: 1) planning for complex goals; and 2) robust execution.

Towards achieving the first goal, the community has adopted activity planning, in which goal satisfaction is achieved by stringing together a sequence of activities from a predefined library. A classic approach was described in [3], although more modern approaches such as [4] allow the satisfaction of temporal as well as spatial specifications. One promising method for activity planning relies on the idea of flow tubes [5], a way to describe the reachability of the state space given an initial position and a chosen activity.

*This work was supported by the National Science Foundation under Grant No. IIS-1017992.

¹Computer Science and Artificial Intelligence Laboratory, Massachusetts Institute of Technology, 32 Vassar St, Cambridge, MA 02139, USA {cfang, williams}@mit.edu

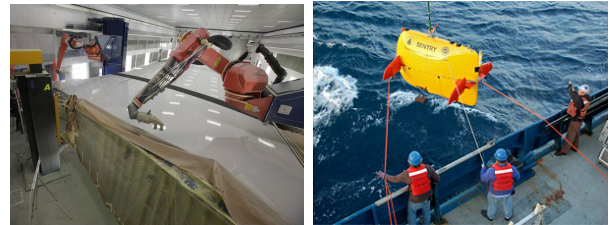


Fig. 1: Both robotic manufacturing and oceanographic surveys with autonomous underwater vehicles require the robust achievement of complex goals. In robotic manufacturing, parts must be assembled in order, and failures to meet goals may result in faulty products. In oceanographic surveys, goals may include spatial and temporal information, required for describing collaborative missions with heterogeneous vehicles, and failures in execution may lead to reduced science return or loss of expensive vehicles.

Robust planning has also been of interest in robotics. Studies into probabilistic planning have traditionally centred around the process based on the Markov Decision Process (MDP) framework [6], with extensions for example to partially observable domains in [7] and to information theoretic approaches for mapping in [8]. There has recently been a shift to robust planning in terms of chance-constraints, in which the resulting policy results in a bounded probability of failure, demonstrated in [9], [10], [11].

A natural combination of the two ideas, resulting in a chance-constrained activity planner, would be of significant importance. A schematic describing the combination of the two ideas is given in Figure 2. However, such a planner must have a way to probabilistically bound the trajectories of the vehicle for reachability analysis. This may be done through propagation of statistics, in which a model of vehicle dynamics is used in conjunction with information about the noise in actuation, to characterise the uncertainty about the state of the vehicle at points in time.

However, characterising the noise is often non-trivial. While the mean and variance of the noise may be determined experimentally, it is often difficult to find the right function to describe the distribution of the noise. One method for dealing with unknown distributions is given in [11]. The accuracy of statistics thus derived are difficult to guarantee, typically coming from convergence and concentration inequalities. A Gaussian assumption is typically made instead.

The Gaussian assumption may not be valid. For example, actuation noise may be bounded on one side. We concentrate on statistics propagation with non-Gaussian actuation noise. In particular, we assume that only the first two moments are

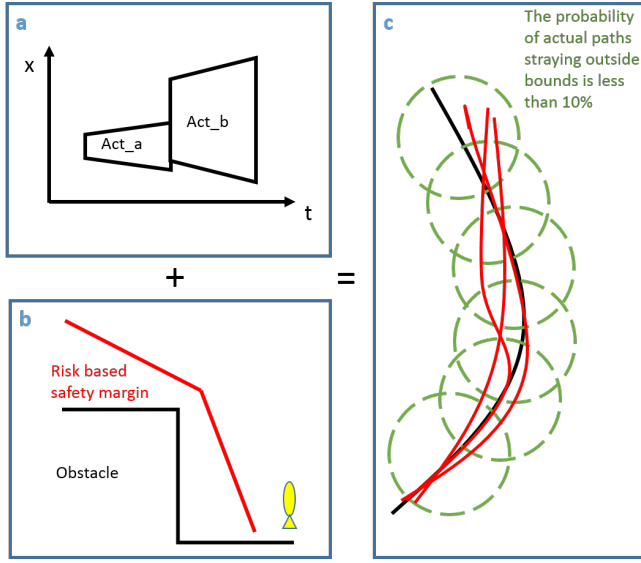


Fig. 2: a) Flow tubes used in activity planning. Complex goals with temporal and spatial dimensions are specified as areas in some state space. Previous work have used flow tubes, each representing an activity from a library, to perform reachability analysis in order to check by construction whether the goals are achievable; b) The idea of chance-constrained programming notes that the risk of failure during a mission may be written as the sum of risks of failure during each point in the mission. Implicit in chance-constrained programming is a way to evaluate the risk of each activity; c) One way to combine the two paradigms, flow tube planning with chance constraints, is a set of bounds on the possible evolution of states during an activity. Instead of reachability, we may instead look at the probability of the state straying beyond the bounds.

known. Apart from the generality this gives us, this is also useful in the case when the noise model was derived from sampling the distribution, since approximations for the first two moments are relatively easy to calculate.

We first note that, when the dynamics are linear functions of the system state and noise, propagation of the first two moments is exact. We also show in simulation that making Gaussian assumptions on the posterior distribution leads to incorrect bounds on the magnitude of the expected error. However, by looking at the expected error squared as a stochastic process, we can show that it is a submartingale under assumptions about dynamics, and use Doob's Inequality to probabilistically bound the magnitude of the expected error over the entire path. While propagation is generally not exact in the nonlinear case, we show in simulation that the unscented transform gives us sufficiently accurate estimates for the mean and covariance, hence allowing us to bound the expected error over the entire path in a similar fashion.

II. LINEAR DYNAMICS

We begin by examining a system with linear dynamics. Consider a discrete time system, with dynamics:

$$\mathbf{x}_{k+1} = f_k(\mathbf{x}_k, \mathbf{u}_k, \mathbf{w}_k) \quad (1)$$

where \mathbf{x}_t , \mathbf{u}_t , and \mathbf{w}_t are the system state, control input and control noise at time step t (all assumed to be column

vectors). Further, assume that we are given the finite first two moments for the distribution \mathbf{w}_t , $E[\mathbf{w}_t] = \mu_t$, $E[(\mathbf{w}_t - \mu_t)(\mathbf{w}_t - \mu_t)^T] = \Sigma_t$, and that the noise between time steps is independent. Note that state noise is *not necessarily Gaussian*, as we allow any distribution which permits a closed form evaluation of the mean and covariance.

Let $\hat{\mathbf{x}}_t = E[\mathbf{x}_t]$ and $Q_t = E[(\mathbf{x}_t - \hat{\mathbf{x}}_t)(\mathbf{x}_t - \hat{\mathbf{x}}_t)^T]$ describe the distribution at time t . We also assume that we have some initial estimate for the system, given as $\hat{\mathbf{x}}_0 = E[\mathbf{x}_0]$ and $Q_0 = E[(\mathbf{x}_0 - \hat{\mathbf{x}}_0)(\mathbf{x}_0 - \hat{\mathbf{x}}_0)^T]$.

Let the dynamics of the system be linear. For A_k, B_k , and C_k finite matrices for every finite time k , we have:

$$f_k(\mathbf{x}_k, \mathbf{u}_k, \mathbf{w}_k) = A_k \mathbf{x}_k + B_k \mathbf{u}_k + C_k \mathbf{w}_k \quad (2)$$

We thus have the propagation equations:

$$\hat{\mathbf{x}}_{k+1} = A_k \hat{\mathbf{x}}_k + B_k \mathbf{u}_k \quad (3)$$

$$Q_{k+1} = A_k Q_k A_k^T + C_k \Sigma_k C_k^T \quad (4)$$

These *exactly* propagate the first and second moments for the random variable \mathbf{x}_k , given the correct moments for initial distribution at $t = 0$.

Given that we have the exact first and second moments for the state at every time step, we would like to be able to characterise the uncertainty in the estimate. For example, we can attempt to apply Gaussian assumptions and probabilistically bound the estimation error at each time step. However, note that given only the mean and covariance of the noise term, we can not in general guarantee that the resulting distribution will be well approximated by a Gaussian.

Consider a 2D system with speed and heading controls. Suppose heading control α_k is noiseless, but given nominal speed \tilde{v}_k , the actual speed v_k is drawn from the distribution:

- With probability 0.05: $v_k = 0$
- With probability 0.95: $v_k \sim \text{Exp}(1/(1.1\tilde{v}_k))$, where $\text{Exp}(1/\mu)$ is an exponential distribution with mean μ

Then, let

$$\mathbf{x}_{k+1} = \mathbf{x}_k + \begin{bmatrix} v_k \cos \alpha_k \\ v_k \sin \alpha_k \end{bmatrix}$$

This may approximate, for example, an underwater vehicle with unreliable propeller control failing with probability 5%.

We may write the dynamics in the form of (2), such that

$$A_k = I \quad B_k = C_k = \begin{bmatrix} \cos \alpha_k \\ \sin \alpha_k \end{bmatrix} \\ \mathbf{u}_k = E[v_k] = 1.045\tilde{v}_k \quad \mathbf{w}_k = v_k - E[v_k]$$

Note that we have translated the noise term. This does not affect the variance, so $\Sigma_k = E[(v_k - E(v_k))(v_k - E(v_k))^T] = 0.95(\tilde{v}_k^2 + 2.2\tilde{v}_k) - E[v_k]^2$. However, $E[\mathbf{w}_k] = 0$. The cumulative distribution function (cdf) of \mathbf{w}_k is given in Figure 3 for nominal speed 10.

Simulating the above system forward, we can obtain Figure 4 as an example. We simulated the vehicle forward for 10 time steps, starting with a zero mean Gaussian distribution for state with 0.01 standard deviation in X and Y. We simulated with constant nominal $\tilde{v}_k = 1$ and constant increase in α_k of $5\pi/180$. We attempted to fit

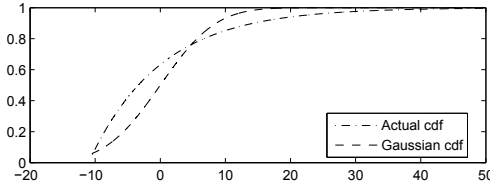


Fig. 3: The cdf of \mathbf{w}_k , in comparison with the cdf of the Gaussian distribution with the same mean and covariance.

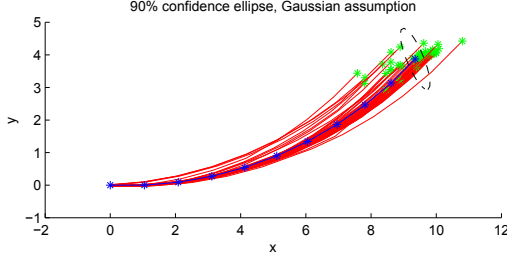


Fig. 4: An example of a forward simulation, with dynamics linear in the state and noise terms. The blue line shows the expected trajectory. The red lines shows the simulated actual trajectories, with the green stars denoting the final locations. The 90% confidence ellipse, assuming Gaussian posterior for final distribution, is shown as the black dashed line. We see that the Gaussian assumption is inappropriate for providing error bounds, as over half of the trajectories end outside the ellipse.

the 90% confidence bound for the end state of the vehicle, assuming Gaussian posterior. It is clear that the estimate is inappropriate. With 5000 forward simulations, 4175 were outside the confidence bounds for the 11th step. Given the sample size the difference is significant. Hence, we can not rely on Gaussian assumptions if we wanted probabilistic guarantees on bounds for the estimation error.

III. SQUARED ERROR AS STOCHASTIC PROCESS

While Gaussian assumptions are generally inappropriate, under some circumstances we are still able to provide probabilistic bounds on the estimation error. Consider the important linear case, where the eigenvalues of A_k are greater than 1. This describes a wide range of systems, for example the vehicle above.

That is, consider the case when we have an unstable system, with the implication that the state uncertainty grows unbounded. Let us now consider the squared error at time k , $Y_k = (\mathbf{x}_k - \hat{\mathbf{x}}_k)^T (\mathbf{x}_k - \hat{\mathbf{x}}_k)$.

We first make the observation that Y_k is non-negative for all k . Further, since we are considering the linear case, we know that \mathbf{x} is a random variable, and hence Y_k is a random variable for each k . Then, we have $\{Y_k\}$ a non-negative discrete time stochastic process. We want to further show that $\{Y_k\}$ is a submartingale, a particular type of stochastic process for which there exists a well-known inequality. We will first give a definition for submartingales, and then prove that $\{Y_k\}$ is a submartingale.

Definition 1: Consider a discrete time process $X = \{X_1, X_2, \dots\}$. X is a submartingale if for all $n < \infty$,

- $E[X_n] < \infty$; and
- $E[X_{n+1} | X_1, X_2, \dots, X_n] \geq X_n$

Theorem 1: $\{Y_k\}$ the sequence of squared errors as defined above is a submartingale.

Proof: Observe first that for each k , $E[Y_k] = \text{trace}(Q_k)$. Given that the matrices A_t , C_t and Σ_t are finite for all time t , and that Q_0 finite, then Q_k finite for finite k , hence $Y_k = \text{trace}(Q_k)$ finite.

For the second requirement, note first that $E[Y_{k+1} | Y_1, Y_2, \dots, Y_k] = E[Y_{k+1} | Y_k]$, since the true state at any time only depends on the true state at the previous time step. Now,

$$\begin{aligned} E[Y_{k+1} | Y_k] &= E[(\mathbf{x}_{k+1} - \hat{\mathbf{x}}_{k+1})^T (\mathbf{x}_{k+1} - \hat{\mathbf{x}}_{k+1}) | Y_k] \\ &= E[(\mathbf{x}_k - \hat{\mathbf{x}}_k)^T A_k^T A_k (\mathbf{x}_k - \hat{\mathbf{x}}_k) \\ &\quad + \mathbf{w}_k^T C_k^T C_k \mathbf{w}_k | Y_k] \end{aligned}$$

Recalling that all eigenvalues of A_k are greater than 1 and that w_k is independent of X_k due to white noise assumption:

$$E[Y_{k+1} | Y_k] \geq Y_k + E[\mathbf{w}_k^T C_k^T C_k \mathbf{w}_k]$$

Hence, we find that $E[Y_{k+1} | Y_k] \geq Y_k$ as required. \blacksquare

Now that we have shown $\{Y_k\}$ to be submartingale, we can leverage theories in stochastic processes to provide bounds on its magnitude. In particular, we can use Doob's Inequality. We state the result without proof below, and refer interested readers to the martingales chapter of [12].

Theorem 2 (Doob's Maximal Inequality): Consider $X = \{X_1, \dots, X_N\}$ a non-negative submartingale. Then,

$$P(X_* \geq \lambda) \leq \lambda^{-1} E[X_N]$$

where $X_* = \max_{i=1, \dots, N} X_i$

We now consider the implications of the above result on error bounding. With a direct application of the Maximal Inequality on the sequence of squared error $\{Y_k\}_{k=1, \dots, N}$, we may find a bound on the estimation error, not just for one particular time step, but *over all time steps*. We illustrate how this may be applied with a bit of motivation.

Suppose we wish to perform chance-constrained planning, where we need to bound the probability of deviating from some predefined path. That is, suppose we want to find some bound R for which the probability of the estimation error being greater than R at any time is less than some Δ . Then, we require:

$$P(\{\exists k \text{ s.t. } |\mathbf{x}_k - \hat{\mathbf{x}}_k| \geq R\}) \leq \Delta$$

or equivalently

$$P(\{\max_k |\mathbf{x}_k - \hat{\mathbf{x}}_k| \geq R\}) \leq \Delta$$

We present the probabilistic bound on the trajectory.

Theorem 3: (Submartingale bound for vehicle trajectory) Consider a linear system described by $\mathbf{x} = A_k \mathbf{x}_k + B_k \mathbf{u}_k + C_k \mathbf{w}_k$, where $|A_k|$, $|B_k|$, and $|C_k|$ finite. Further, suppose that the eigenvalues of A_k are *greater than 1*. Let Q_N be the covariance at the final time step. Then,

$$P(\{\max_k |\mathbf{x}_k - \hat{\mathbf{x}}_k| \geq R\}) \leq R^{-2} \text{trace}(Q_N)$$

		1% Bound	5% Bound	10% Bound	20% Bound	30% Bound
Prob of propeller failure 1%	Gaussian assumption bounds	3247	4543	5699	7203	8329
	Submartingale bounds	0	19	90	1329	1920
Prob of propeller failure 5%	Gaussian assumption bounds	5325	7262	8331	9914	10907
	Submartingale bounds	0	3	73	676	1264
Prob of propeller failure 10%	Gaussian assumption bounds	7060	9552	10855	12531	13653
	Submartingale bounds	0	2	39	417	1188
Maximum expected		200	1000	2000	4000	6000

TABLE I: The number of trials out of 20000 in which the path error was greater than the probabilistic submartingale bounds, for linear dynamics described in (2).

for any $R \in \mathbb{R}$.

Proof: We retain the definition of Y_k , and observe that

$$P(\{\max_k |\mathbf{x}_k - \hat{\mathbf{x}}_k| \geq R\}) = P(\{\max_k Y_k \geq R^2\})$$

Recall that $\{Y_k\}$ is a submartingale. Let $Y_* = \max_{k=1, \dots, N} Y_k$. By applying Doob's inequality, we find:

$$P(Y_* \geq R^2) \leq R^{-2} E[Y_N]$$

As $E[Y_N] = \text{trace}(Q_N)$, we have the required inequality. ■

The above result gives us a way to find confidence regions for the state of the vehicle at every time step. We are able to upper bound the probability of the state error becoming greater than a set value. Specifically, assume we require $P(\{\exists k \text{ s.t. } |\mathbf{x}_k - \hat{\mathbf{x}}_k| \geq R\}) \leq \Delta$. We can let $R^{-2} \text{trace}(Q_N) = \Delta$ to enforce the bound. We may thus choose

$$R = \sqrt{\Delta^{-1} \text{trace}(Q_N)} \quad (5)$$

This bound is also remarkable because it is dependent only on the final covariance: the initial uncertainty of the path is irrelevant as long as the trace of the final covariance is the same. It is also more powerful than Chebyshev's Inequality. The same error bound is provided not just for one particular time step, but for all time steps. Intuitively, both of these properties come from the additional information given to us by the form of the stochastic process, that the conditional expectation of the next path error is related to the current path error.

Consider the scenario discussed in the previous section. We simulate forward with the same parameters for speed and heading. In one set of trials, we start with standard deviation in X and Y of 0.01 each as before, and in the second with standard deviation in X and Y of 0.1 each. The sample results and the probabilistic bounds derived from Doob's Inequality are plotted in Figure 5, and compared with the bounds from the Gaussian assumption.

Visually, we can confirm from Figure 5 that most of the simulated outcomes do lie within the bounds derived using the maximal inequality, whereas the Gaussian assumptions are inappropriate. To check that this is consistent across a number of scenarios, we performed additional numerical simulations, using the described linear dynamics with a faulty propeller.

We varied the parameter denoting the probability of propeller failure, and calculated the bounds from varying chance constraints. For each combination of parameters we

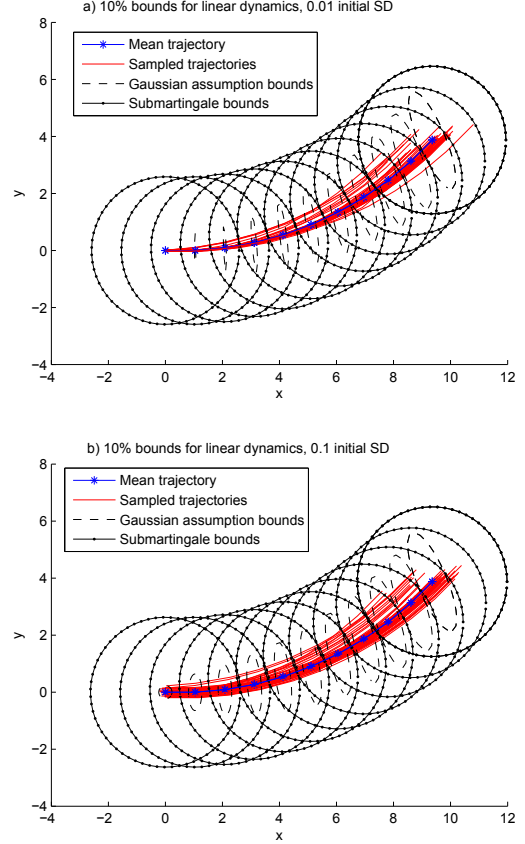


Fig. 5: Example forward simulations, with dynamics linear in the state and noise terms. The mean and sampled trajectories are shown, together with the bounds on the trajectories at each time step from Gaussian assumption and from the maximal inequality. The Gaussian assumption is again inappropriate, as can be seen by considering the distribution of the end points.

generated 20000 trials, where each trial involved a set of 10 randomly generated heading control drawn uniformly from the interval $[-0.5\pi, 0.5\pi]$. We counted the number of trials in which the largest path error was greater than the probabilistic bounds derived using the submartingale inequality. We compare the performance of the submartingale bound against that of the Gaussian assumption, used in state of the art chance-constrained planning [10]. The results are summarised in Table I.

As demonstrated in the trials, the bounds derived from the submartingale maximal inequality were correct, as opposed to those from applying the Gaussian assumption, in the sense

that the percentage of actual paths deviating beyond the bounds were less than the corresponding risk bounds. We know that the bounds are necessarily loose; after all, we assume we did not have any information in addition to the first two moments of the actuation noise. The bounds must thus be large enough to cover a variety of distributions with the same first and second moments.

Note that as the risk allowance gets higher, the bounds become less loose. The sampled trajectories are not as spread out. Though we are taking more risk by using a smaller radius for our trajectory bound, we are still meeting the chance-constraint.

IV. NONLINEAR SYSTEMS

The above bounds on estimation error were derived for systems with dynamics linear in the state and noise terms. In particular, linearity was used to ensure that the second moment was propagated exactly, and to prove that the squared error was a submartingale. We would like to be able to make predictions in the nonlinear case, and provide similar probabilistic bounds given only the first and second moments.

Unfortunately, in general there does not exist closed form methods for exact propagation of first and second moments. The discussion in the appendix of [13] provides good reasons for why simply maintaining the first two moments will not be sufficient for exact propagation of first and second moments for state estimates. In this sense, we can not provide rigorous theoretical guarantees for bounds on the estimation error as we did in the linear case.

Note, however, that the unscented transform [13] was designed to perform good approximations of the first two moments with the choice of sigma points. Further, observe that for common nonlinear systems, without measurement updates the estimated error seems to increase with time. This motivated us to attempt to fit probabilistic bounds for the nonlinear case, with the first and second moments obtained through unscented transform.

Consider now a dynamic system with three elements in the state vector, representing XY and heading, and speed and heading change inputs. Suppose the speed input behaviour is as before, and that the heading input $d\theta_k$, for nominal heading change $\hat{d}\theta_k$, is drawn uniformly from the interval $[\hat{d}\theta_k - \frac{\pi}{180}, \hat{d}\theta_k + \frac{\pi}{180}]$. Then, using a Dubin's "car" model [14], we may have the transition function:

$$\begin{bmatrix} x_{k+1} \\ y_{k+1} \\ \theta_{k+1} \end{bmatrix} = \begin{bmatrix} x_k + v_k \cos(\theta_k + 0.5d\theta_k) \\ y_k + v_k \sin(\theta_k + 0.5d\theta_k) \\ \theta_k + d\theta_k \end{bmatrix} \quad (6)$$

Note that again, the actuation noise distributions are not Gaussian. The non-Gaussian actuation noise and the nonlinear dynamics means that we can not use normal Gaussian assumptions to bound the path errors, motivating the use of particle filter [15]. We argue that we can still provide bounds for path error, using the technique above, with only the first and second moments the distribution.

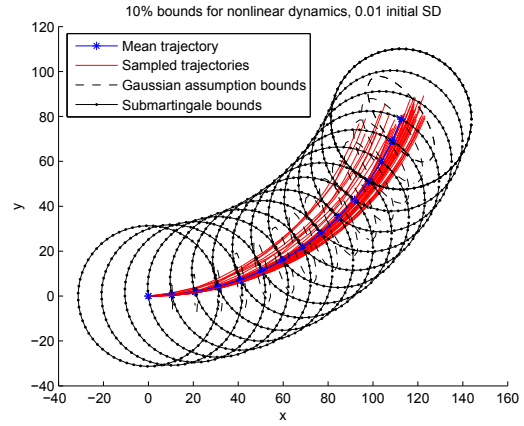


Fig. 6: Examples of a forward simulations with nonlinear dynamics described in (6). Statistics were propagated using the unscented transform. Again, we plot the mean of the trajectory and sampled trajectories, along with the 10% bounds for derived from Gaussian assumptions and the maximal inequality.

Since transition is nonlinear in the noise terms, we also included the terms in selection of sigma points. Specifically, at time k , for sigma points $\sigma^{(i)}$, $i = 1, \dots, 10$, we had

$$\begin{aligned} \sigma^{(0)} &= [\mathbf{x}_k; E[v_k]; E[d\theta]]^T \\ \Sigma &= \begin{bmatrix} Q_k & 0 & 0 \\ 0 & E[(v_k - E[v_k])^2] & 0 \\ 0 & 0 & E[(d\theta - E[d\theta])^2] \end{bmatrix} \end{aligned} \quad (7)$$

By then propagating the sigma points forward with the dynamics above, we expect a good estimate of the mean and covariance. Note that, as in the linear case, we only used the first and second moments for noise in the propagation equations, and do not assume any other information about the distributions are given. Again, we consider the trace of the final covariance, and determine a probabilistic bound. Simulations were performed with a zero mean Gaussian initial distribution with standard deviation 0.01 in all three state element, and statistics were propagated for 10 steps, with nominal speed 10, and heading change $\frac{5\pi}{180}$. Example paths and the probabilistic bounds are presented in Figure 6.

Again, the figure seems to suggest that the bounds are correct. Similar to the linear case, we performed additional numerical simulations, using the new nonlinear dynamics. As before, we varied the probability of propeller failure, and calculated bounds for varying amounts of risk. For each set of parameters detailed in Table II, 20000 trials were again generated, where each trial involved a set of 10 randomly generated expected control angles drawn uniformly from the interval $[-0.5\pi, 0.5\pi]$. We counted the number of trials in which the largest path error was greater than the corresponding bound derived using the submartingale inequality.

The probabilistic bounds remain correct in the sense that the percentage of path deviations greater than the bound was less than that specified in all cases, and the Gaussian

		1% Bound	5% Bound	10% Bound	20% Bound	30% Bound
Prob of propeller failure 1%	Gaussian assumption bounds	13758	15279	16012	16789	17249
	Submartingale bounds	0	15	111	1322	2005
Prob of propeller failure 5%	Gaussian assumption bounds	12290	13978	14878	16060	16603
	Submartingale bounds	0	2	84	744	1311
Prob of propeller failure 10%	Gaussian assumption bounds	16691	17817	18308	18776	19031
	Submartingale bounds	0	1	38	467	1167
Maximum expected		200	1000	2000	4000	6000

TABLE II: The number of trials out of 20000 in which the path error was greater than the probabilistic submartingale bounds, for nonlinear dynamics described in (6).

assumption remain inappropriate. The probability that the vehicle strays outside the trajectory bounds derived was indeed less than that required. However, we note again the conservatism of the bounds, although again conservatism seems to become more reasonable for the larger risk bounds, for the same reasons as before.

V. CONCLUSION

The vision for robotic planning is ultimately a planner which generates controls to robustly achieve complex goals. This would have wide-ranging applications, from manipulation for manufacturing to oceanographic science missions. In recent times, promising research has focused separately on activity planning for complex missions, and chance-constrained programming for robust execution. A necessary component in a combination of the two approaches is a way to probabilistically bound the evolution of the state through the execution of the activity.

Our major contributions in this work are:

- We proved that, under assumptions, the path error throughout the duration of an execution may be considered a submartingale;
- Using well-known results from stochastic processes, we were able to derive probabilistic bounds on the trajectories for both linear and nonlinear dynamics.

We began by looking at forward propagation of statistics, given only the first and second moments, and derived probabilistic error bounds. It was shown empirically that Gaussian assumptions do not always work well, even when the statistics are propagated exactly in the linear case. Instead, we showed that, for the linear case, the error squared is a submartingale. This allowed us to fit a error bound, not only on the estimation error at a single time step, but for all time steps, using only the final covariance. Although, we lose the guarantees of exact propagation in the nonlinear case, we noted that we may still propagate the first two moments of the probability distribution in state using the unscented transform. We showed through simulation that the probabilistic bound calculated using the final covariance resulting from the unscented transform seems correct for nonlinear systems.

A. Future work

This work has made some head way into error bounds for propagation, with only mean and covariance information about the actuation noise distribution. This was demonstrated in simulation with a linear system and a nonlinear system,

with non-Gaussian noise. While the former confirmed the theory, and the latter seems to support engineering intuition, perhaps a more in depth study is merited, with a greater range of noise and dynamics models. It must also be noted that the bounds derived were loose. However, in the absence of more information about the distribution other than the first two moments, in general it is difficult to improve on Doob's inequality. Given more information (bounded increments for example), we may reasonably leverage other concentration inequalities, and provide tighter bounds on estimation error.

REFERENCES

- [1] S. Dong and B. Williams, "Motion learning in variable environments using probabilistic flow tubes," in *Robotics and Automation (ICRA), 2011 IEEE International Conference on*. IEEE, 2011, pp. 1976–1981.
- [2] R. Camilli, C. M. Reddy, D. R. Yoerger, B. A. Van Mooy, M. V. Jakuba, J. C. Kinsey, C. P. McIntyre, S. P. Sylva, and J. V. Maloney, "Tracking hydrocarbon plume transport and biodegradation at deep-water horizon," *Science*, vol. 330, no. 6001, pp. 201–204, 2010.
- [3] E. Frazzoli, "Robust hybrid control for autonomous vehicle motion planning," Ph.D. dissertation, Massachusetts Institute of Technology, 2001.
- [4] S. Karaman and E. Frazzoli, "Sampling-based motion planning with deterministic μ -calculus specifications," in *Decision and Control, 2009 held jointly with the 2009 28th Chinese Control Conference. CDC/CCC 2009. Proceedings of the 48th IEEE Conference on*. IEEE, 2009, pp. 2222–2229.
- [5] H. Li and B. Williams, "Hybrid planning with temporally extended goals for sustainable ocean observing," in *AAAI*, 2011.
- [6] R. S. Sutton and A. G. Barto, *Reinforcement learning: An introduction*. Cambridge Univ Press, 1998, vol. 1, no. 1.
- [7] L. P. Kaelbling, M. L. Littman, and A. R. Cassandra, "Planning and acting in partially observable stochastic domains," *Artificial intelligence*, vol. 101, no. 1, pp. 99–134, 1998.
- [8] H. Geffner and B. Bonet, "High-level planning and control with incomplete information using pomdps," in *Proceedings Fall AAAI Symposium on Cognitive Robotics*, 1998.
- [9] L. Blackmore and M. Ono, "Convex chance constrained predictive control without sampling," in *Proceedings of the AIAA Guidance, Navigation and Control Conference*, 2009.
- [10] M. Ono, B. C. Williams, and L. Blackmore, "Probabilistic planning for continuous dynamic systems under bounded risk," *Journal of Artificial Intelligence Research*, vol. 46, pp. 511–577, 2013.
- [11] M. C. Campi and S. Garatti, "A sampling-and-discarding approach to chance-constrained optimization: feasibility and optimality," *Journal of Optimization Theory and Applications*, vol. 148, no. 2, pp. 257–280, 2011.
- [12] R. Durrett, *Probability: theory and examples*. Cambridge university press, 2010, vol. 3.
- [13] S. J. Julier and J. K. Uhlmann, "Unscented filtering and nonlinear estimation," *Proceedings of the IEEE*, vol. 92, no. 3, pp. 401–422, 2004.
- [14] S. M. LaValle, *Planning algorithms*. Cambridge university press, 2006.
- [15] M. S. Arulampalam, S. Maskell, N. Gordon, and T. Clapp, "A tutorial on particle filters for online nonlinear/non-gaussian bayesian tracking," *Signal Processing, IEEE Transactions on*, vol. 50, no. 2, pp. 174–188, 2002.